PERGAMON

Chemical Engineering Science 57 (2002) 977–990

Chemical Engineering Science

www.elsevier.com/locate/ces

Analysis of transient thickness of pneumatic foams

Laurent Pilon[a], Andrei G. Fedorov[b], Raymond Viskanta[a,*]

[a] *Heat Transfer Laboratory, School of Mechanical Engineering, Purdue University, West Lafayette, IN 47907-1288, USA*
[b] *Multiscale Integrated Thermofluidics Laboratory, Woodruff School of Mechanical Engineering, Georgia Institute of Technology, GA 30332-0405, USA*

Received 12 June 2001; received in revised form 29 October 2001; accepted 19 November 2001

Abstract

This paper presents a simple, experimentally validated approach to analyze the transient formation of a foam layer produced by injecting gas bubbles into a foaming solution. Based on experimental observations, three different regimes in the transient growth of the foam have been identified as a function of the superficial gas velocity. A model based on the mass conservation equation for the gas phase in the foam combined with three different models for the average porosity is proposed. It is shown that for practical calculations a constant average porosity equal to 0.82 can be used. The model predictions show very good agreement with experimental data for low superficial gas velocity and provide an upper limit of the foam thickness for intermediate and large superficial gas velocities. The paper discusses the physical mechanisms that may occur during the foam formation and the effects of the superficial gas velocity on the foam dynamics. The present analysis speculates several mechanisms for the bursting of the bubbles at the top of the foams and proposes the framework for more fundamental and detailed studies.

Keywords: Foam; Multiphase flow; Separations; Food processing; Modelling; Porous media

1. Introduction

Pneumatic or semi-batch foams are produced by a continuous stream of gas bubbles rising to the surface of a foaming liquid. Such foams are encountered in a number of practical technological systems ranging from chemical and materials processing, to protein separation and bioreactors. Bubbles are either generated by chemical reactions taking place within the liquid or injected into the liquid through a single nozzle, a multinozzle inlet or a porous medium.

In electric arc furnaces, foam is often required to shield the refractories from the arc, to protect the liquid metal from the atmosphere (Ozturk & Fruehan, 1995) and to help stabilize the arc in modern electric arc furnaces (Ozturk & Fruehan, 1995). In many other applications such as chemical reactors or food processing, the foam is undesirable. In glass melting furnaces, bubbles produced by chemical reactions taking place within the melt accumulate at the surface of the glass melt and form a foam layer that reduces significantly heat transfer rates from the combustion space to the melt (Laimbock, 1998; Kappel, Conradt, & Scholze, 1987; Fedorov & Viskanta, 2000), thereby increasing the operating temperature, the NO_x-formation rate, and the energy consumption (Laimbock, 1998). The transient behavior of foams is of particular importance for processes that require constant adjustment of the operating parameters to meet the production needs. For example, in glass melting furnaces, operators have to constantly adapt the pull rate, the feeding of the batch and the firing rate as a function of the production needs. Such changes affect the foam layer thickness that grows or decays accordingly.

Understanding and modelling of the transient foam thickness is, therefore, of major importance from both fundamental and practical viewpoints. The objective of the present work is to develop a model for predicting the thickness of a foam layer during its formation, i.e., between the beginning of the gas injection until the foam reaches a steady state.

2. Current state of knowledge

2.1. Foam structure

Foams consist of an ensemble of bubbles of different sizes. The bubble size distribution at the bottom of the foam layer

* Corresponding author. Tel.: +1-765-494-5632; fax: +1-765-494-0539.
E-mail address: viskanta@ecn.purdue.edu (R. Viskanta).

0009-2509/02/$ - see front matter
PII: S0009-2509(02)00010-6

depends on the injection systems (Narsimhan & Ruckenstein, 1986a). Bubbles can take different shapes and polyhedral and spherical bubbles often coexist within the foam layer. The polyhedral bubbles tend to be located at the top of the foam while the spherical ones are at its bottom (Malysa, 1992; Hutzler, Weaire, & Shah, 2000). Even though polyhedral bubbles can adopt different geometries, they all obey a few rules known as the Plateau's laws (Bhakta & Ruckenstein, 1997): (i) three and only three films meet at an edge at an angle of 120°, (ii) four and only four edges (Plateau border channels) meet at a point at an angle of 109°. It has been observed that a regular dodecahedron nearly satisfies Plateau's laws and is considered as an idealized polyhedral bubble.

2.2. Physical phenomena

Several physical phenomena occur simultaneously or consecutively as the foam is generated. These phenomena are as follows:

(i) *Gravity drainage* of the liquid through the Plateau borders opposed by the viscous forces.
(ii) *Drainage* of the liquid in the films driven by the capillary pressure due to the curvature of the adjacent Plateau channels and opposed by the disjoining pressure consisting of the Van der Waals attractive forces, the repulsive electrical double layer and the hydration forces (Bhakta & Ruckenstein, 1997). Drainage in the foam eventually stops when the effect of the capillary forces (or Plateau border suction) balances the effect of gravity (Bhakta & Ruckenstein, 1997; Krotov, 1981).
(iii) *Coalescence* of two adjacent bubbles as a result of the rupture of the film separating them. Coalescence causes the mean bubble size to increase and the number of bubbles as well as the interfacial area of the foam to decrease.
(iv) *Interbubble gas diffusion* [1] from small bubbles (higher pressure) to large bubbles (lower pressure). This causes the small bubbles to become smaller and the large bubbles to become larger provided that the solubility and the diffusion coefficient of the gas in the liquid phase are large enough. A theoretical analysis by Narsimhan and Ruckenstein (1986b) indicates that interbubble gas diffusion is significant only at the top of the foam where the bubble lamellae are thin.
(1) Gibbs–Marangoni effect in thin liquid films and foams results in a decrease of the surface excess surfactant concentration caused by stretching an interface, hence in an increase in surface tension (Gibbs effect); the surface tension gradient thus created causes liquid to flow toward the stretched region, thereby providing both a "healing" force and also a resisting force against further thinning (Marangoni effect).

[1] Also called Ostwald ripening or disproportionation.

It has been observed for different types of liquid phases (molten glass, Laimbock (1998) and aqueous solutions, Barber and Hartland (1975)) that bubbles do not necessarily burst when the lamellae reach their critical thickness. Instead, they remain in a so-called metastable state until they burst. Thus, the rupture of lamellae occurs due to two independent and consecutive processes. The first stage in the rupture of the film is its thinning due to drainage, and the second stage is the tear of the film probably due to random molecular collisions (Djabbarah & Wasan, 1985). According to Hrma (1990), the lifetime of a bubble cannot be determined from the thickness of its lamellae, and the characteristic time of rupture can be expressed as a function of two characteristic times: (i) the characteristic time of drainage τ_d, and (ii) the lifetime of the critically thin film τ_c (Djabbarah & Wasan, 1985; Hrma, 1990):

$$\tau = \tau_d + \tau_c. \tag{1}$$

The lifetime τ_c depends on the properties of the fluid and on the bubble radius, but it is independent of the gas supply (Hrma, 1990). If $\tau_c = 0$, the foam is said to be evanescent, that is, bubbles burst as soon as their lamellae reach the critical thickness. In general, τ_c is non-zero and the foam is said to be metastable (Hrma, 1990).

2.3. Foam porosity

As a result of gravity drainage, the foam becomes "dryer" and the porosity, defined as the ratio of the local volume of gas to the volume of foam, increases from the bottom to the top of the foam layer. It is usually assumed (Narsimhan & Ruckenstein, 1986a, b; Bhakta & Ruckenstein, 1997) that the porosity at the bottom of the foam is constant with time and equals 0.74 corresponding to the maximum packing of spherical bubbles of the same size. In reality, the porosity varies with time from zero as bubbles start reaching the surface of the liquid to its steady-state value. Hartland and Barber (1974) have observed that even though the liquid holdup close to the liquid/foam interface varies with time, it rapidly reaches a steady state while the foam is still growing. In other words, the characteristic time for the porosity at the bottom of the foam required to reach a steady state is negligible compared to that of the foam thickness. Therefore, the assumption that the porosity at the bottom of the foam is constant with time is an acceptable approximation.

2.4. Modelling

Several models describing the transient behavior of pneumatic foams are available in the literature and have been reviewed recently (Bhakta & Ruckenstein, 1997). Most of them consist of solving a system of differential equations for the foam thickness and for the local foam porosity or the liquid hold-up (Bhakta & Ruckenstein, 1997; Narsimhan, 1991). The fundamental governing equation called "the drainage equation" is based on the local mass conservation

of the liquid phase (Bhakta & Ruckenstein, 1997). The one-dimensional formulation of the drainage equation in terms of the foam porosity at height z and time t, $\phi(z,t)$, is written as follows (Bhakta & Ruckenstein, 1997):

$$\frac{\partial \phi}{\partial t} = \frac{\partial}{\partial z}(\phi q_{PB}), \tag{2}$$

where q_{PB} is the volumetric flux of the liquid phase through the Plateau border channels at location z and time t. Assuming that (1) the foam bed consists of dodecahedron bubbles of the same size, (2) the Plateau borders are randomly oriented, (3) the drainage through the Plateau borders due to film thinning is negligible compared to that due to gravity [see Bhakta and Ruckenstein (1997), Narsimhan (1991) for additional discussion], (4) coalescence of bubbles and Ostwald ripening within the foam are absent, (5) surface tension is constant, (6) the wall effects are negligible, and (7) the foam is under isothermal conditions, an expression for the volumic flow rate through the Plateau border $q_{PB}(z,t)$ is given by (Pilon, Fedorov, & Viskanta, 2001)

$$q_{PB}(z,t) = 3.632 \times 10^{-3} c_v \frac{[1-\phi(z,t)]^2}{\phi(z,t)} \times \left\{ \frac{\rho g r^2}{\mu} + \frac{1.3957}{\alpha} \frac{\sigma r^2}{\mu} \frac{\partial}{\partial z} \times \left[\left(\frac{\phi(z,t)}{(1-\phi(z,t))r^2} \right)^{1/2} \right] \right\}, \tag{3}$$

where ρ is the liquid density, μ is the liquid viscosity, σ is the surface tension of the gas/liquid system, and r is the bubble radius. In this equation $\alpha = \sqrt{0.644}/0.322$, and the velocity coefficient c_v (dimensionless) accounts for the mobility of the walls of a Plateau border channel and has been computed by Desai and Kumar (1982). In most of their calculations, Ruckenstein and coworkers used $c_v = 1$ (Bhakta & Ruckenstein, 1997). The initial porosity distribution in the foam and two boundary conditions are needed to solve Eqs. (2) and (3). The porosity at the bottom of the foam layer $\phi(z_2,t)$ is traditionally assumed to be constant and equal to 0.74 and the volumetric flux q_{PB} is assumed to be zero at the top of the foam (Germick, Rehill, & Narsimhan, 1994; Bhakta & Ruckenstein, 1995). Two approaches have been used to determine the initial porosity in the studies of the decay of standing foams. Narsimhan (1991) used a quasi-steady-state model to compute the initial porosity as a function of the location in the pneumatic foam. His analysis is based on the assumption that the loss of liquid by gravity drainage is compensated by the liquid entrained with the rising bubbles. On the other hand, Bhakta and Ruckenstein (1995) solved the drainage equation using moving boundaries during the foam formation. The latter model compares better with experimental data for the decay of pneumatic foams than the quasi-steady-state approach indicating that "the unsteady nature of foam formation cannot be ignored" (Bhakta & Ruckenstein, 1995). Thus, the solution for foam decay has been proven to be highly sensitive to the initial bubble size distribution in the foam (Bhakta & Ruckenstein, 1997). However, it is difficult to obtain or predict the initial bubble size distribution either experimentally, analytically or numerically (Monsalve & Schechter, 1984; Bhakta & Ruckenstein, 1997).

More sophisticated models have been proposed that account for coalescence of bubbles as well as interbubble gas diffusion and require the solution of an additional equation for the local average film thickness of the lamellae as a function of position in the foam (Bhakta & Ruckenstein, 1997; Narsimhan & Ruckenstein, 1986b). These models assume that the neighboring bubbles coalesce as soon as the thickness of the lamellae reaches the critical film thickness, i.e., the foam is assumed to be evanescent.

Another possible approach to deal with transient behavior of foams is the use of population balance theory. Narsimhan and Ruckenstein (1986a) developed such a model accounting for drainage, coalescence, and interbubble gas diffusion. Drainage is treated assuming dodecahedron bubbles while the treatment of interbubble gas diffusion is based on spherical bubbles. Such assumptions have been judged to be inevitable given the complexity of the system, and this model is difficult to extend to transient problems (Bhakta & Ruckenstein, 1997). More recently, Hartland and co-workers Ramaswami, Hartland, & Bourne, 1993; Hartland, Bourne, & Ramaswami, 1993) have developed a transient population balance equation by accounting for drainage and interbubble gas diffusion and neglecting coalescence. However, the population balance equations available in the literature for bubbles in foams (Narsimhan & Ruckenstein, 1986a; Ramaswami et al., 1993) assume that the number density function is smooth, differentiable with respect to time and space coordinates [see Ramkrishna (2000) for more details]. In other words, "the population balance equation is to be viewed as an averaged equation" (Ramkrishna, 2000) that is valid when the population is large enough to consider its behavior as deterministic, i.e., the deviation about the average is negligible (Ramkrishna, 2000). However, the validity of the above-mentioned models (Narsimhan & Ruckenstein, 1986a; Ramaswami et al., 1993) can be questionable in the upper part of the foam where only a small number of bubbles is present. For such small populations a stochastic approach seems to be more appropriate (Ramkrishna, 2000) but is not available in the literature.

Even though the physical phenomena taking place in the formation of a foam layer appear to have been identified and are qualitatively understood, the modelling of the transient behavior of pneumatic foams have been concerned mainly with the decay of standing foams (Bhakta & Ruckenstein, 1997, 1995; Narsimhan & Ruckenstein, 1986b; Barber & Hartland, 1975; Narsimhan, 1991; Germick et al., 1994). One should also mention that parametric studies of the transient and steady-state foam behaviors have been performed (Bhakta & Ruckenstein, 1997), but very little validation

against experimental data has been reported (Germick et al., 1994; Bhakta & Ruckenstein, 1995).

Moreover, all the models assume that bubbles are dodecahedron in shape and are continuously bursting at the top of the foam layer. Although such assumptions are valid for the decay of standing foams, they are difficult to justify during the foam formation, particularly at an early stage (Bhakta & Ruckenstein, 1997). The polyhedral shape assumption does not account for the fact that as drainage, coalescence and Ostwald ripening take place, the foam porosity increases from 0.74 to values close to unity, requiring the bubble to change from spherical to polyhedral shape. Such a change in shape is particularly important in the transient formation of the foam.

Finally, the observation that the solution of the model equations for the foam decay available in the literature are highly dependent on the initial conditions provides an additional motivation for studying the formation of the foam layer from a liquid surface free of foam to a steady-state foam layer.

In the present work, an attempt is made to develop a simple model for predicting the transient thickness of a foam layer generated by bubbling a gas in a foaming solution. A simple yet physically sound approach based on the first principles is preferred to the solution of a complex system of differential equations accounting for drainage, bubble coalescence, and interbubble gas diffusion.

3. Analysis

Following Hartland and Barber (1974), the experimental data for the formation of pneumatic foams can be classified into three different types of transient behavior depending on the superficial gas velocity (see Fig. 1 for illustration):

(1) For low superficial gas velocity, the foam thickness increases almost linearly with time until it reaches a steady state. Small and slow transient fluctuations of the foam thickness around the steady-state thickness are observed.
(2) For intermediate superficial gas velocity, the foam thickness increases almost linearly with time until the foam gets into a cycle of successive collapse and growth. Unlike the previous type, the fluctuations of the foam thickness with time are such that one cannot consider the foam as being at a steady state. Note that as the flow rate increases, the oscillations tend to be smoother but their amplitude remains significant. Hartland and Barber (1974) divided this type of transient behavior into two different regimes: the first one characterized by sudden oscillations, and the second one characterized by smoother oscillations. Here, we do not make the distinction since the overall behavior is similar, i.e., no apparent steady state can be defined due to large oscillations of the foam thickness with time.
(3) For large superficial gas velocity, the foam thickness increases almost linearly with time but after some time the foam breaks down into a froth (Hartland & Barber, 1974). The froth height is lower than that of the foam for similar conditions. Hartland and Barber (1974) attributed this to turbulence and other factors that cause the film at the top of the foam to rupture at greater thicknesses. At higher gas flow rates, no foam is observed and the dispersion becomes a froth immediately as indicated by Hartland and Barber (1974).

Experimental data do not permit the definition of a general criteria between the three different transient behaviors. Such a criteria would depend on the thermophysical properties of the liquid and gas phases, on the superficial gas velocity, on the container size and shape, and on other factors.

3.1. Mass conservation equation

In this section, we present a model for predicting the foam thickness as a function of time during the foam generation. The analysis uses the following simplifying assumptions:

(1) The problem is one-dimensional and transient, i.e., the foam porosity is a function of time and vertical position only (Bhakta & Ruckenstein, 1997).
(2) The wall effects are negligible.
(3) The foam is isothermal.
(4) During the transient formation of the foam layer, no bubbles burst at the surface of the foam.

Let us consider a container of constant cross-sectional area S containing a solution at rest as schematically represented in Fig. 2. Initially (i.e., at $t = 0$), gas bubbles are injected at the bottom of the container at a constant superficial gas velocity j. We also assume that the gas flux j is large enough to generate foam. Let $H(t)$ be the height of the foam at any time t. The coordinate system is chosen with the origin located at the top of the foam as shown in Fig. 2.

According to the above assumptions, the mass conservation of the gas phase within the foam can be expressed as

$$\frac{\mathrm{d}m_g(t)}{\mathrm{d}t} = \rho_g j S \quad \text{if } t \leqslant \tau, \tag{4}$$

where ρ_g is the density of the gas phase, j the volumetric gas flux or superficial gas velocity, and τ is the time for the foam thickness to reach a steady state. The total mass of gas retained within the foam $m_g(t)$ can be expressed as a function of the gas density ρ_g and the foam porosity $\phi(z,t)$:

$$m_g(t) = \int_0^{H(t)} \rho_g \phi(z,t) S \,\mathrm{d}z. \tag{5}$$

Assuming that the gas density and the container area are constant, Eqs. (4) and (5) can be combined and simplified to become

$$H(t)\bar{\phi}(t) = jt \quad \text{if } t \leqslant \tau, \tag{6}$$

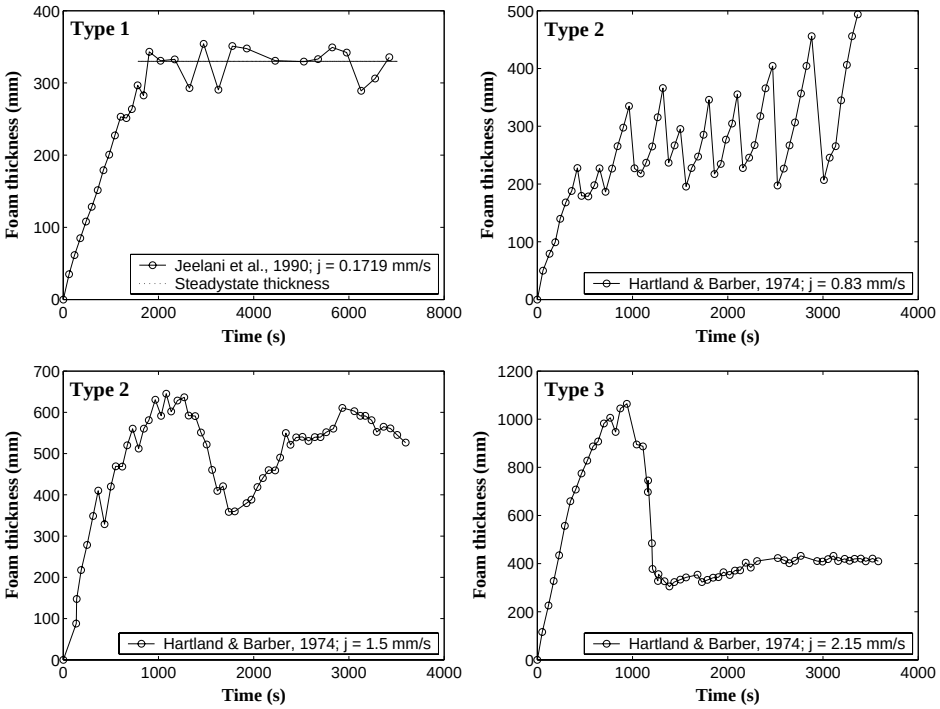

Fig. 1. Different types of transient during foam formation.

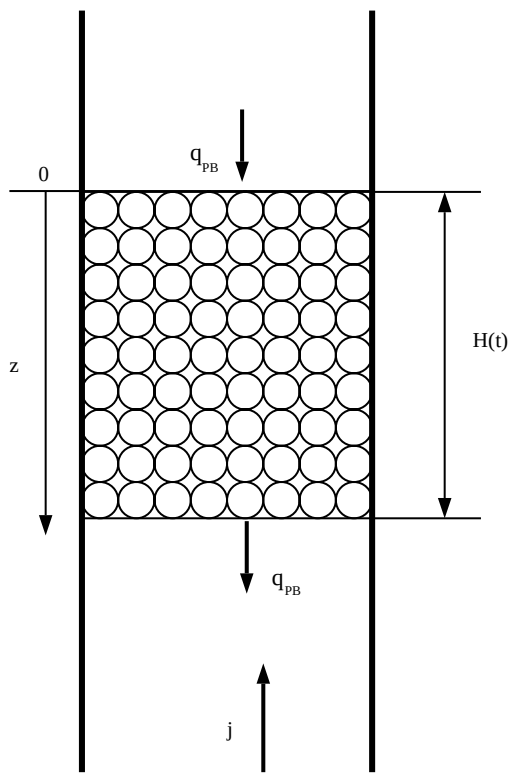

Fig. 2. Schematic of a foam layer generated by bubbling and coordinate system with notations.

where $\bar{\phi}(t)$ is the instantaneous average foam porosity defined as

$$\bar{\phi}(t) = \frac{1}{H(t)} \int_0^{H(t)} \phi(z,t)\,\mathrm{d}z. \tag{7}$$

According to Eq. (6), the transient foam thickness can be predicted if one knows the evolution of the instantaneous average (over height) foam porosity $\bar{\phi}(t)$ with time.

3.2. Porosity profile

In this section, we develop an approximate expression for the porosity profile in the foam layer as a function of time t and location z. We choose a second-order polynomial to represent the local porosity distribution $\phi(z,t)$:

$$\phi(z,t) = a_0 + a_1 \left[\frac{z}{H(t)}\right] + a_2 \left[\frac{z}{H(t)}\right]^2, \tag{8}$$

where the coefficients a_0, a_1, and a_2 are generally functions of time, unless self-similar solution is obtained. Three conditions are needed to determine these three coefficients and they are obtained from the boundary conditions at the top and bottom of the foam layer:

$$\phi[H(t),t] = \phi_2, \tag{9}$$

$$\phi(0,t) = \phi_1(t), \tag{10}$$

$$\left.\frac{\partial \phi(z,t)}{\partial z}\right|_{z=0} = 0. \tag{11}$$

Eq. (9) states that the porosity at the bottom of the foam is constant, as previously discussed, and is taken as 0.74 corresponding to the maximum packing of spherical bubbles of identical size. Eq. (10) indicates that the porosity at the top of the foam is a function of time only. The third condition [Eq. (11)] reflects the fact that, in most cases, drainage of liquid occurs in the lower part (bottom) of the foam layer and this eventually stops at the top of the foam layer when the gradient of the capillary pressure balances the gravity force (Bhakta & Ruckenstein, 1997; Krotov, 1981). Then, only coalescence may cause the foam porosity to increase at the top of the foam (Bhakta & Ruckenstein, 1997), but it is speculated to occur only when the foam is sufficiently drained and the lamella thickness is less than about 100 nm (Narsimhan & Ruckenstein, 1986b). The drainage flow rate induced by the rupture of the foam lamellae is extremely small, thereby making the porosity $\phi(z,t)$ change very little and, thus, the partial derivative $\partial\phi(z,t)/\partial z$ can be assumed to vanish at the top of the foam (i.e., at $z=0$) as given by Eq. (11). Several models and numerical simulations of the foam liquid holdup using boundary conditions different from Eq. (11) (Desai & Kumar, 1983; Narsimhan & Ruckenstein, 1986b; Bhakta & Ruckenstein, 1997) have been presented in the literature. They all predict that "the liquid holdup decreases rapidly near the foam/pool liquid interface and less in the rest of the [foam] bed" (Narsimhan & Ruckenstein, 1986b). Predicted porosity profiles computed for foaming solutions with different viscosity, surface tension, and bubble radius indicate that Eq. (11) is a reasonable first-order approximation. It should be noted that the boundary conditions [Eq. (11)] can also be deduced by using the well-known condition of zero velocity or zero flow rate of the liquid though the Plateau borders at the top of the foam [i.e., $q_{PB}\ (z=0,t)=0$] (Bhakta & Ruckenstein, 1997). In addition, it must be assumed that the radius does not change with the location z and the porosity is unity at the top of the foam layer.

Using the boundary conditions, Eqs. (9)–(11) and solving Eq. (8) for the parameters a_0, a_1, and a_2 results in the following porosity profile within the foam:

$$\phi(z,t)=\phi_1(t)+[\phi_2-\phi_1(t)]\left[\frac{z}{H(t)}\right]^2. \tag{12}$$

The average foam porosity corresponding to this profile can be computed using Eq. (7):

$$\bar{\phi}(t)=\frac{2\phi_1(t)+\phi_2}{3}. \tag{13}$$

At the beginning of the foam growth, the bottom and the top of the foam are superimposed and the gas volume fraction at the top of the foam is similar to that at the bottom. As the foam grows and gravity drainage takes place, the porosity at the top increases until the thickness of the lamellae and the porosity at the top reach their respective critical values for which bubbles start bursting. Moreover, Jeelani, Ramaswami, and Hartland (1990) reported porosity values at the top of the foam approaching unity for steady-state foams. Therefore, it is believed that $\phi_1(t)$ varies between ϕ_2 at the beginning of the foam formation and its maximum values taken as unity at steady state.

The next step in the present analysis is to model the evolution of $\phi_1(t)$ and thus $\bar{\phi}(t)$ with time. Three different models are considered in the following sections: the average porosity is (i) constant with time, (ii) an exponential function of time, and (iii) obtained by approximate solution of the drainage equation.

(i) *Constant porosity at the top*

The simplest approach is to assume that the porosity at the top of the foam $\phi_1(t)$ does not change with time and equals the arithmetic mean of its minimum and its maximum values. In agreement with the experimental observations, we assume that $\phi_{1,\min}=0.74$ and $\phi_{1,\max}\approx 1.0$. In this case $\phi_1(t)$ is taken to be 0.86, and according to Eq. (13) the average foam porosity is $\bar{\phi}(t)=0.82$.

(ii) *Exponential variation of ϕ_1 with time*

The characteristic time for reaching the steady-state foam thickness should be identical to the characteristic time for the porosity at the top of the foam to reach a critical value beyond which bubbles start bursting at the top. Let τ be the characteristic time for the foam thickness to reach a steady state, then the change of the porosity $\phi_1(t)$ with time can be expressed as

$$\phi_1(t)=\phi_{1,\max}+(\phi_{1,\min}-\phi_{1,\max})\mathrm{e}^{-t/\tau}. \tag{14}$$

The value for τ can be obtained by solving Eq. (6) for the case $H(t=\tau)=H_\infty$ where H_∞ is the steady-state foam thickness:

$$\tau=\frac{\bar{\phi}(\tau)H_\infty}{j}$$

$$=\frac{H_\infty}{j}\left\{\frac{2}{3}\phi_{1,\max}+(\phi_{1,\min}-\phi_{1,\max})\mathrm{e}^{-1}+\frac{1}{3}\phi_2\right\}. \tag{15}$$

Again, assuming that $\phi_2=\phi_{1,\min}=0.74$ and $\phi_{1,\max}=1.0$, we obtain

$$\tau=\frac{0.85H_\infty}{j}. \tag{16}$$

An expression for the steady-state thickness H_∞ can be found in the literature for foams generated from high-viscosity fluids (Pilon et al., 2001). Two dimensionless numbers have been identified as describing the effect of surface tension, viscosity, density, bubble radius, and superficial gas velocity (Pilon et al., 2001). However, all the experimental data for transient foam behavior collected from the literature are concerned with low-viscosity solutions, and nitrogen is used as the filling gas, except for one set of experimental data reported by Hartland et al. (1993) who used xenon. But, according to Pilon et al. (2001), in the case of nitrogen bubbled in low-viscosity solutions, the

same approach as that used for high-viscosity solutions can be used. Thus, a correlation for the steady-state thickness of foams generated by bubbling nitrogen into low-viscosity solutions has been developed using the two dimensionless parameters previously mentioned:

$$\frac{H_\infty}{r_0} = \frac{213,177}{Ca}\left(\frac{Fr}{Re}\right)^{1.77}, \tag{17}$$

where Re, Fr, and Ca are the Reynolds, Froude and Capillary numbers, respectively, defined as

$$Re = \frac{\rho_c(j-j_m)r_0}{\mu}, \quad Fr = \frac{(j-j_m)^2}{gr_0}, \quad Ca = \frac{\mu(j-j_m)}{\sigma}, \tag{18}$$

here j_m is the superficial gas velocity for onset of foaming, μ is the viscosity of the foaming solution, r_0 is the radius of the bubbles at the bottom of the foam, and σ is the surface tension. Since all the experimental data sets for transient foam thickness except one were obtained by bubbling nitrogen in low-viscosity solutions, the value of the steady-state foam thickness can be substituted into Eq. (15) to give the following expression for τ as the function of the thermophysical properties and the superficial gas velocities:

$$\tau = 1.812\times10^5\,\frac{\sigma}{jr_0^{2.54}}\,\frac{[\mu(j-j_m)]^{0.77}}{(\rho g)^{1.77}}. \tag{19}$$

Finally, having determined the characteristic time for the foam to reach a steady state τ, the average foam porosity can be expressed as a function of time t, $\phi_{1,\min} = 0.74$, and $\phi_{1,\max} = 1.0$, as follows:

$$\bar{\phi}(t) = 0.91 + 0.17e^{-t/\tau}. \tag{20}$$

(iii) *Approximate solution of the drainage equation*

The drainage equation [Eqs. (2) and (3)] is solved approximately by the series method (Tenenbaun & Pollar, 1963) using the following boundary conditions:

$$\phi[H(t),t] = \phi_2, \tag{21}$$

$$q_{PB}(0,t) = 0, \tag{22}$$

where q_{PB} is the volumetric flux of the liquid phase through the Plateau border channels at location z and time t. Note that at the top of the foam the velocity of the fluid through the Plateau border due to gravity drainage must be zero since no liquid enters the foam at the top (Bhakta & Ruckenstein, 1995), therefore, $q_{PB}(0,t) = 0$. Integrating Eq. (2) with respect to the space variable from $z = 0$ to $z = H(t)$ and using the above boundary conditions together with the Leibnitz rule yields

$$\frac{\mathrm{d}}{\mathrm{d}t}\left(\int_0^{H(t)}\phi\,\mathrm{d}z\right) - \phi_2\,\frac{\mathrm{d}H(t)}{\mathrm{d}t} = \phi_2 q_{PB}[H(t),t], \tag{23}$$

where $q_{PB}[H(t),t]$ is the flux of liquid through the Plateau borders at the foam/liquid interface. Substituting the expression for the average porosity $\bar{\phi}(t)$ given by Eq. (7) into Eq. (23) leads to the following differential equation:

$$\frac{\mathrm{d}}{\mathrm{d}t}(\bar{\phi}H) - \phi_2\,\frac{\mathrm{d}H}{\mathrm{d}t} = \phi_2 q_{PB}[H(t),t]. \tag{24}$$

The flux of liquid through the Plateau borders at the foam/liquid interface $q_{PB}[H(t),t]$ can be found by substituting Eq. (12) into Eq. (3) and assuming that $\phi_2 = 0.74$ and the change in the bubble radius with location is negligible, then Eq. (24) becomes

$$H\,\frac{\mathrm{d}}{\mathrm{d}t}(\bar{\phi}H) - 0.74H\,\frac{\mathrm{d}H}{\mathrm{d}t} = AH - B(\phi_1(t) - 0.74), \tag{25}$$

where

$$A = 2.46\times10^{-4}c_v\,\frac{\rho g r^2}{\mu}, \tag{26}$$

$$B = 1.10\times10^{-2}c_v\,\frac{\sigma r}{\mu}. \tag{27}$$

Eq. (25) has two unknowns [$\bar{\phi}(t)$ and $H(t)$]. Thus, one needs an additional equation to complete the problem formulation. One can use Eq. (6) to obtain the following system of equations for $\bar{\phi}(t)$ and $H(t)$ as dependent variables:

$$\frac{\mathrm{d}}{\mathrm{d}t}(\bar{\phi}H) = j, \tag{28}$$

$$H\,\frac{\mathrm{d}}{\mathrm{d}t}(\bar{\phi}H) - 0.74H\dot{H} = AH - \frac{3}{2}B(\bar{\phi} - 0.74). \tag{29}$$

The initial conditions are:

$$\bar{\phi}(t=0) = \phi_2, \tag{30}$$

$$H(t=0) = 0. \tag{31}$$

Integrating Eq. (28) and substituting the expression for the foam thickness $H(t)$ ($=jt/\bar{\phi}$) into Eq. (29) yields

$$j^2t\bar{\phi}(\bar{\phi} - 0.74) + 0.74j^2t^2\,\frac{\mathrm{d}\bar{\phi}}{\mathrm{d}t} = Ajt\bar{\phi}^2 - \frac{3}{2}B(\bar{\phi} - 0.74)\bar{\phi}^3. \tag{32}$$

We now have a single non-linear first-order ordinary differential equation [Eq. (32)] that can be solved approximately or numerically.

An approximate solution for early times of the foam formation is sought using the series method (Tenenbaun & Pollar, 1963). We assume that the average porosity $\bar{\phi}(t)$ can be expressed as a Taylor series during the initial phase of the foam formation (i.e., t is small):

$$\bar{\phi} = \sum_{i=0}^{\infty} b_i t^i. \tag{33}$$

Substituting this expression in Eq. (32) and identifying the first three terms in t^i gives

$$b_0 = \phi_2, \quad b_1 = \frac{2}{3}\left(\frac{Aj}{B\phi_2}\right), \quad b_2 = -j\phi_2(A + 2j)b_1. \tag{34}$$

The Taylor series in Eq. (33) needs to be truncated for practical calculations. If only the first two terms are retained, the approximate solution of the low $O(1)$ order could be only obtained and this approximation is valid as long as the time interval is between 0 and $o(b_1/b_2)$. On the other hand, if more precise solution with a second order of approximation [e.g., $O(2)$] is sought, the first three terms in the series need to be retained in Eq. (33), albeit this more precise solution is valid over much shorter time interval between $t = 0$ and $o(b_2/b_3)$. Unfortunately, the upper limit of time for validity of the second-order approximation [i.e., $o(b_2/b_3)$] is a very small number (tenths of a second), and no experimental data fall into this time interval to warrant any further discussion and use of the second-order approximation. Thus, the cruder first-order model (i.e., $\phi = b_0 + b_1 t$) that is valid for a much longer time interval is used in this study to provide meaningful comparison with available experimental data.

4. Results and discussion

4.1. Validation against experimental data

4.1.1. Low superficial gas velocity

Fig. 3 shows typical experimental data for the transient foam thickness with the type 1 behavior obtained with a nitrogen flux of $j = 0.1719$ mm/s in a solution of 10% glycerine + water + 80 mg/l of Marlophen-89 (Jeelani et al., 1990). The predictions of Eq. (6) are also plotted by assuming an average porosity $\bar{\phi}$ of 0.74 and 0.91. As one can see, the experimental data fall between these two extreme cases. The assumption that no bubbles burst at the surface of the foam during the transient growth is valid for transients of type 1. It appears that the steady-state thickness is reached shortly after the mass conservation equation for the gas phase [Eq. (6)] is no longer satisfied. The only possible reason for the equation not to be valid is if the bubbles at the top of the foam start bursting or if the gas contained in the bubble at the top of the foam diffuses to the atmosphere. However, the sudden change in the transient foam thickness toward its steady-state value indicates that the responsible phenomena is abrupt and suggests that the bursting of the bubbles at the top is a major event causing the foam to rapidly reach a steady-state thickness.

It is also interesting to note that at the early stage of the foam formation, the experimentally measured thickness follows Eq. (6) with $\bar{\phi} = 0.74$ and, at a later stage, it tends toward the predictions of Eq. (6) with $\bar{\phi} = 0.91$. Similar plots were obtained for other type 1 transients. This can be explained by the fact that as the liquid phase leaves the foam at the bottom as a result of drainage, the average porosity increases causing the slope $\mathrm{d}H/\mathrm{d}t$ to slightly decrease with time. At the same time, the bubbles change from spherical to polyhedral shape.

Figs. 4–6 compare the experimental data (see Table 1) for the transient foam thickness in the case of the low superficial gas velocity with the predictions of the present work obtained with the three different models previously presented. Good agreement is obtained for all three models and particularly when the average porosity is assumed constant and equal to 0.82. Note that there were not enough data at the beginning of the foam formation to fully assess the validity of the approximate solution of the drainage equation which is valid when the time t is small. Moreover, as observed in Fig. 3, the experimental data fall within the predictions of Eq. (6) using the extreme values for $\bar{\phi}$ of 0.74 and 0.91, and the difference between the predictions of the two limiting cases is relatively small. Therefore, even the simplest models expressed in terms of average quantities (e.g., porosity) will produce sufficiently accurate results even though it ignores

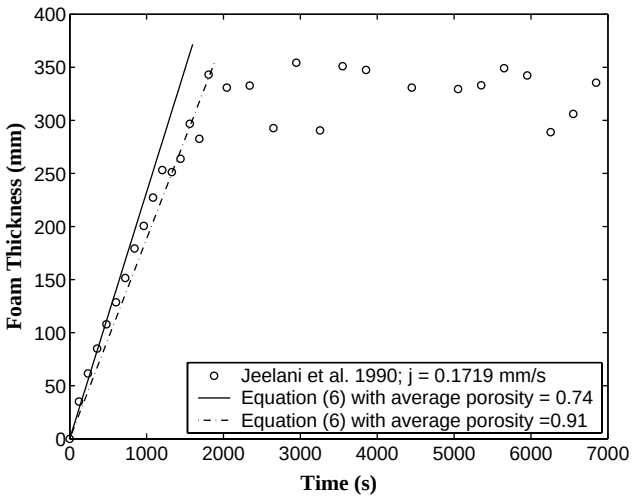

Fig. 3. Comparison between the predictions equation (6) using the limiting values for the average porosity $\bar{\phi}$ and typical experimental data for nitrogen flux $j = 0.1719$ mm/s in 10% glycerine + water + 80 mg/l of Marlophen-89, (Jeelani et al., 1990).

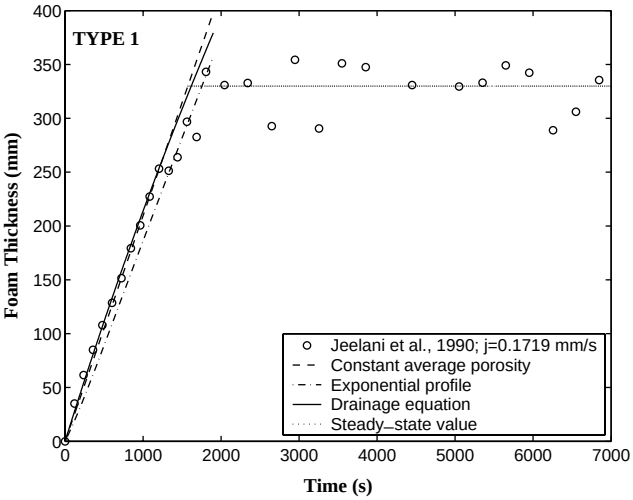

Fig. 4. Comparison of the model predictions with experimental data for nitrogen flux of $j = 0.1719$ mm/s in 10% glycerine + water + 80 mg/l of Marlophen-89 (Jeelani et al., 1990).

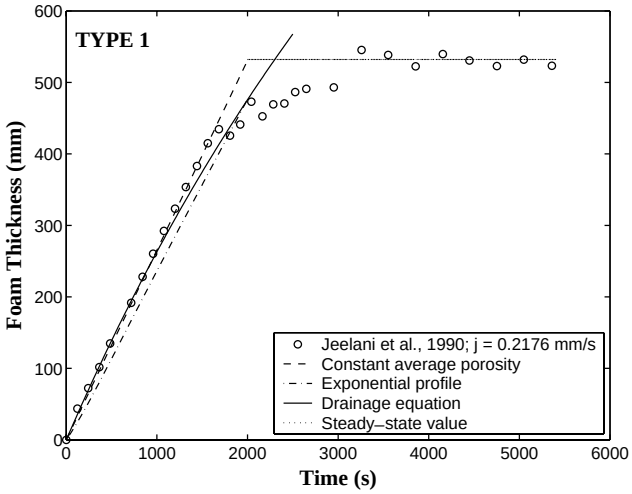

Fig. 5. Comparison of the model predictions with experimental data for nitrogen flux of $j = 0.2176$ mm/s in 10% glycerine + water + 80 mg/l of Marlophen-89 (Jeelani et al., 1990).

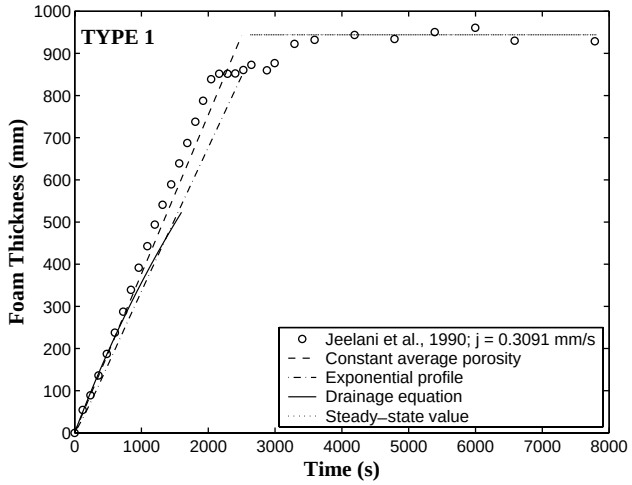

Fig. 6. Comparison of the model predictions with experimental data for nitrogen flux of $j = 0.3091$ mm/s in 10% glycerine + water + 80 mg/l of Marlophen-89 (Jeelani et al., 1990).

some key physical processes taking place during foam formation (e.g., coalescence and Ostwald ripening). Consequently, a simpler approach is preferred and for practical purposes, the average foam porosity can be taken as constant and equal to 0.82.

Fig. 7 shows the average foam porosity deduced from experimental data for low superficial gas velocities by using Eq. (6). A maximum value of 0.91 was imposed when the foam thickness reaches a steady state. It is worth noting that the typical variation with time of the average porosity features a sharp increase in the early stage of the foam formation, then a plateau follows where it does not change significantly, and finally an increase toward its maximum value. This can be explained by the fact that at the beginning, the foam formation is dominated by drainage due to gravity which eventually stops when balanced by the capillary forces (Plateau border suction effects). The foam internal structure does not change significantly for a certain length of time until some films rupture within the foam. The plateau may be due to the stochastic character of film rupture requiring a random time for the first film to rupture. Then, coalescence and drainage of the broken films through the Plateau border channels take place making the average foam porosity increase again. Note that such an analysis is traditionally applied to the foam porosity (Bhakta & Ruckenstein, 1997) at a given location, but it seems that it is also valid for the average foam porosity. All the models reported in the literature (Bhakta & Ruckenstein, 1997; Narsimhan & Ruckenstein, 1986a, b; Narsimhan, 1991) describe drainage, coalescence, and interbubble gas diffusion as occurring simultaneously and continuously in the foam layer. According to Fig. 7, this hypothesis does not seem to be valid for foam formation. Gravity drainage dominates initially during the formation of the foam layer. However, only a few experimental data are available to fully assess the validity of the drainage equation during the drainage-dominated regime of the foam formation. Only when the films separating the bubbles are thin enough, coalescence and interbubble gas diffusion can occur (Narsimhan & Ruckenstein, 1986b). Therefore, the first part of the transient foam formation would consist of gravity drainage only while the second part should depend on gravity drainage and coalescence, as well as interbubble gas diffusion.

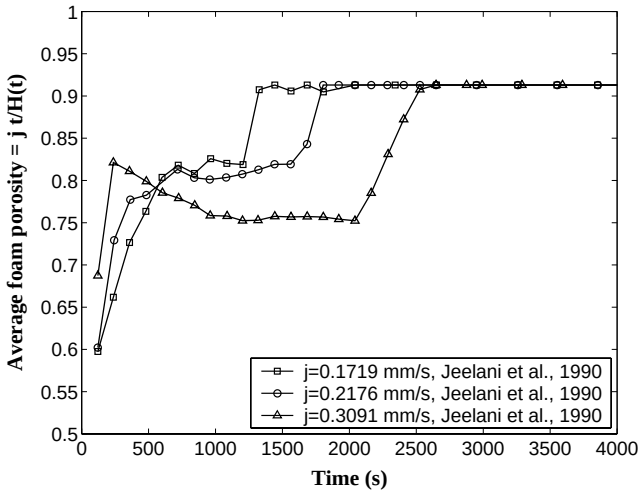

Fig. 7. Evolution of the average porosity with time for nitrogen flux of $j = 0.2176$ mm/s in 10% glycerine + water + 80 mg/l of Marlophen-89 (Jeelani et al., 1990).

Moreover, two different characteristic times for drainage and film rupture or coalescence within the foam seem to prevail and can be measured from Fig. 7. The first increase in the average porosity corresponds to the drainage only and appears to be the same for the three different cases, i.e, the characteristic time for drainage (τ_d) is independent of the superficial gas velocity. The duration of the plateau, i.e., the lifetime of the critically thin film (τ_c), however, seems to

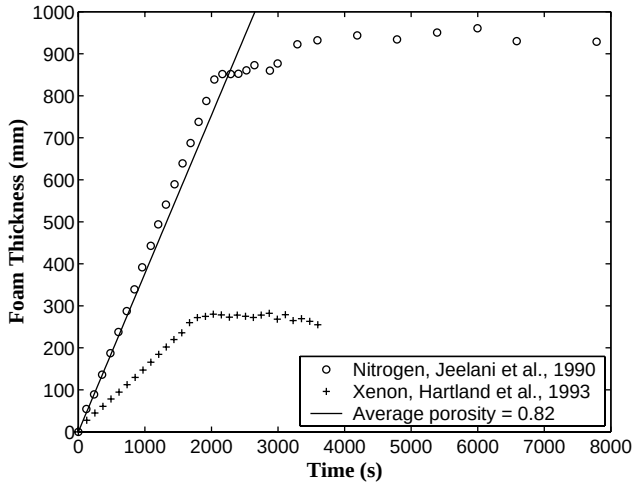

Fig. 8. Comparison of the evolution of the foam thickness with time for nitrogen and xenon flux of $j = 0.3091$ mm/s in 10% glycerine + water + 80 mg/l of Marlophen-89 (Jeelani et al., 1990).

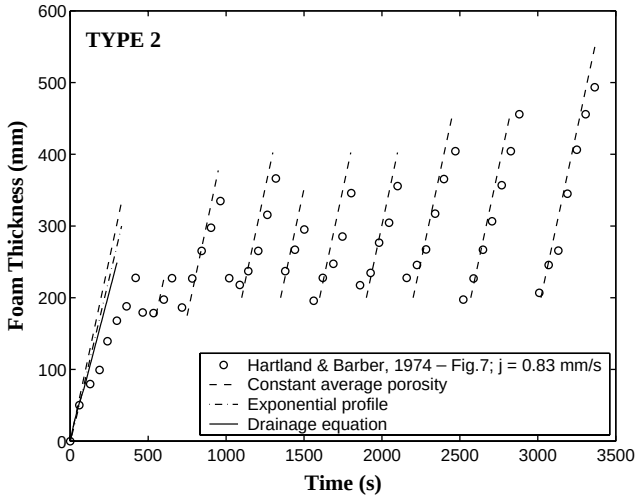

Fig. 9. Evolution of the foam thickness with time for nitrogen flux of $j = 0.83$ mm/s in a solution containing 800 g sucrose, 0.52l glycerol, 1l distilled water, 600 mg/l aerosol OT (Hartland & Barber, 1974).

increase with the superficial gas velocity. This may be due to the fact that as the superficial gas velocity increases, the foam thickness increases and acts as a cushion protecting the bubbles already drained in the upper part of the foam from disturbances occurring at the liquid/foam interface. The larger the superficial gas velocity, the thicker is the absorbing "cushion". Note also that according to Fig. 7, the characteristic time for drainage is significantly smaller than the lifetime for the critically thin film.

To assess the effect of the gas contained is the bubble, only two experimental data sets were found in the literature. Jeelani et al. (1990) and Hartland et al. (1993) reported the variation of the foam thickness with time for a superficial gas velocity of $j = 0.3091$ mm/s in a solution of 10% glycerine + water containing 80 and 120 mg/l of Marlophen-89 and with nitrogen and xenon as the filling gas, respectively. According to Eq. (6) both systems should behave identically since the superficial gas velocity is the same. However, Fig. 8 shows that when xenon is injected into the solution the transient foam thickness deviates significantly from the predictions of Eq. (6), whereas this equation is valid for nitrogen. Even though the amount of surfactant added to the solution is different, the differences in surface tension, density or viscosity between the two solutions are negligible [see Pilon et al. (2001) for a summary of the thermophysical properties]. Therefore, the difference in the transient behavior can only be explained by the type of gas injected into the solutions. Detailed analysis of the physical properties of nitrogen and xenon reported by Hartland et al. (1993) indicates that xenon and nitrogen have similar diffusion coefficients in the liquid phase, but the solubility of xenon is seven times larger than that of nitrogen. Furthermore, Hartland et al. (1993) reported that the Sauter mean diameter increases sharply from the bottom to the top of the foam when xenon is injected while it does not change

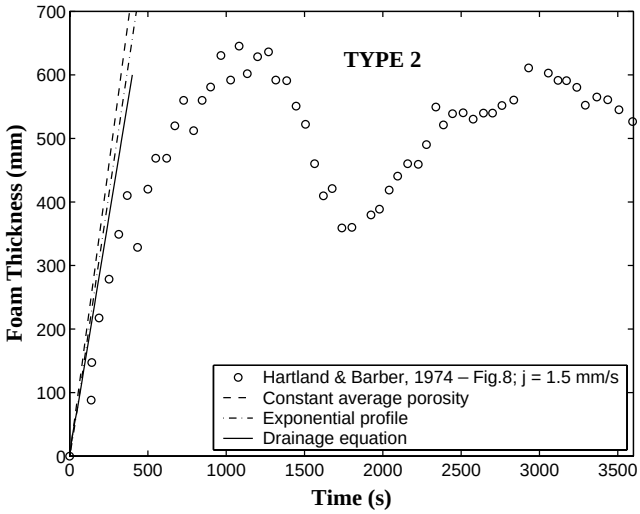

Fig. 10. Evolution of the foam thickness with time for nitrogen flux of $j = 1.5$ mm/s in a solution containing 800 g sucrose, 0.52l glycerol, 1l distilled water, 600 mg/l aerosol OT (Hartland & Barber, 1974).

significantly with nitrogen. This can be explained by the enhanced mass transfer from smaller to larger bubbles as the solubility increases. As suggested by Hartland et al. (1993), the interbubble gas diffusion occurring with xenon leads to larger and more unstable bubbles at the top of the foam that tend to burst faster leading to an early deviation from Eq. (6). For high solubility gases, Ostwald ripening and bursting of the bubbles at the top of the foam should be accounted for to obtain correct predictions of foam dynamics.

4.1.2. Intermediate and large superficial gas velocity

Figs. 9–10 show the evolution of the foam thickness with time for intermediate superficial gas velocity. One can see

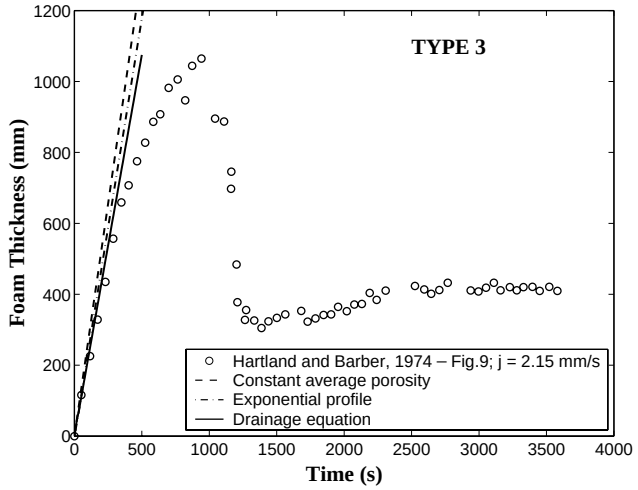

Fig. 11. Comparison of the model predictions with experimental data for nitrogen flux of $j=2.15$ mm/s in a solution containing 800 g sucrose, 0.52l glycerol, 1l distilled water, 600 mg/l aerosol OT (Hartland & Barber, 1974).

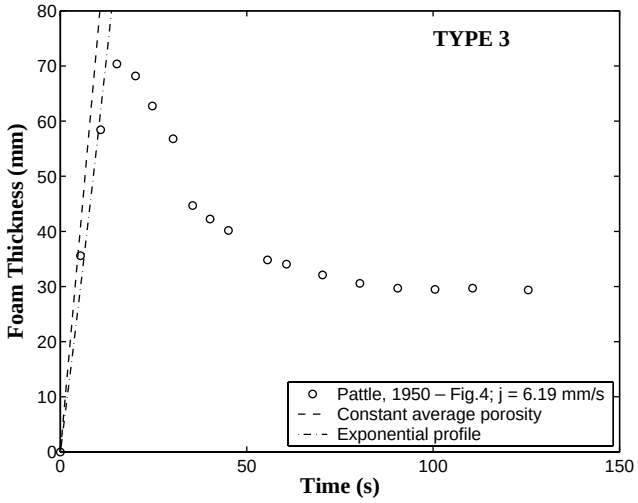

Fig. 12. Evolution of the foam thickness with time for nitrogen flux of $j=6.2$ mm/s in 0.3% gum arabic+1.5% isobutyl alcohol in water solution (Pattle, 1950).

that the model predictions deviate from the experimental data. More precisely, the bubbles at the top of the foam seem to collapse before the foam reaches a steady state. This is believed to be due to the larger gas flow rates that create disturbances in the liquid and at the liquid/foam interface causing the film at the top of the foam to rupture at larger thicknesses. This phenomena is amplified for large superficial gas velocity where foam changes quickly to a steady state froth as suggested by Hartland and Barber (1974) (see Figs. 11 and 12). Therefore, transients of type 2 feature a bifurcating behavior between two possible steady states: (i) steady-state foam and (ii) steady-state froth. Oscillations of the foam thickness with time at intermediate superficial gas velocity are discussed in the next section.

4.2. Oscillations of the foam thickness with time

For low superficial gas velocity (type 1), the steady-state foam thickness oscillates slightly around its mean value, but it was not possible to identify any periodicity, possibly, due to a small sampling rate. However, for intermediate superficial gas velocity (type 2) it is believed that the foam thickness oscillates significantly due to the discrete character of the bubble rupture at the top of the foam (Table 1). Several mechanisms explaining such a behavior can be suggested:

(1) The first bubble bursting at the top of the foam generates a high-velocity liquid jet that breaks up into a number of small drops as observed for a single bubble bursting at a free surface (Boulton-Stone & Blake, 1993). Those drops, when falling back on top of the foam, cause the bubbles sufficiently drained to burst almost simultaneously in a chain reaction. Note that this rupture mechanism has been observed for small single bubbles [<5 mm in diameter, Boulton-Stone and Blake (1993)] bursting at the free surface of a liquid. No jet was observed for large bubbles indicating that the pressure inside the bubble has to be high enough to generate a jet that later breaks up into drops (Boulton-Stone & Blake, 1993). Moreover, the collapse of standing foams has been observed to be discontinuous (Barber & Hartland, 1975), and $H(t)$ is a step function rather than a continuous function of time (Barber & Hartland, 1975). The stages of collapse were longer for higher surface tension and lower viscosity (Barber & Hartland, 1975). This can be explained in terms of the proposed mechanism, by virtue of the fact that the viscosity tends to slow down the jet due to viscous dissipation (Boulton-Stone & Blake, 1993), and the surface tension increases the energy released when the bubbles burst. Note that in the experimental data set reported in Figs. 4 and 6 (Jeelani et al., 1990), the mean diameter of the bubbles at the top of the foam increases with the superficial gas velocity but remains <3.2 mm indicating that the bubbles could generate a jet when bursting.

(2) The first bubble bursting at the top of the foam creates a pressure wave (detonation) propagating through the foam. The magnitude of the detonation depends on the bubble size and is larger for small bubbles since their inside pressure is larger than that of large bubbles. The viscous forces limit the propagation of the pressure wave and a larger surface tension increases the amplitude of the detonation.

For both mechanisms the bubbles that still have thick lamellae can stand the disturbance and act as a protection

Table 1
Summary of experimental conditions for studies reported in the literature and concerned with transient foam thickness

Solution	Dimensions I.D. and H_0	Gas	Gas flux (mm/s)	σ (mN/m)	μ (mPa s)	ρ (kg/m^3)	T ($^\circ$C)	r_0 (mm)	Foam type	References
Water + sucrose AR+ glycerol SLR + aerosol OT	I.D. = 6.15 cm H_0 = N.A.	N_2	0. to 0.82	26	20	1220	30	3.9	1, 2, and 3	Hartland and Barber (1974)
Water + 10% glycerinate Marlophen-89 and 812	I.D. = 10 cm H_0 = 45 cm	Xe	0.31	31.52	1.22	1014	20	0.4	1	Hartland et al. (1993)
Water + 10% glycerinate Marlophen-89 and 812	I.D. = 10 cm H_0 = 45 cm	N_2	0.09 to 0.3091	32.0 to 41.1	1.22	1014	20	0.5 to 0.78	1	Jeelani et al. (1990)
0.3% gum arabic + water +1.5% isobutyl alcohol		Air	6.2	260	N/A	N/A	Room temp.	0.7 to 1.0	3	Pattle (1950)

preventing the entire foam from collapsing. This is confirmed by experimental observation on cells cultivated in a bioreactor that undergo severe damages due the burst of small bubbles close to the free surface (Boulton-Stone & Blake, 1993). However, the damage is significantly reduced in the presence of a slowly draining foam covering the free surface of the reactor (Boulton-Stone & Blake, 1993). For low superficial gas velocities and as observed in Figs. 4–6, oscillations around the steady-state thickness tend to decrease as the superficial gas velocity increases. Similarly, for intermediate superficial gas velocity (type 2 transients), the oscillations are larger for smaller superficial gas velocity as shown in Figs. 9 and 10, even though no steady state can be observed. This can be explained by the fact that as the superficial gas velocity increases, the steady-state foam thickness increases as well as the residence time of the bubbles in the foam allowing them to coalesce more. Thus, increasing the superficial gas velocity causes the bubbles at the top to increase in diameter and their inside pressure to decrease. Hence, the rupture of large bubbles does not trigger the burst of other bubbles as much as does the rupture of smaller bubbles. For thick foams, the bubbles at the top of the foam have a large mean diameter and their rupture can be considered as an isolated event that may generate neither a jet nor a strong detonation. Therefore, the oscillations of the foam thickness become smoother as the superficial gas velocity increases. The major difference between type 1 and type 2 transients can be attributed to the agitation in the liquid phase at the foam/liquid interface that increases with higher superficial gas velocity.

It is interesting to note (in Fig. 9) that during the first few instants of the foam thickness growth, the experimental data deviate significantly from the predictions of Eq. (6), i.e., bubbles start bursting soon after the beginning of the foam formation. At some point in time the foam suffers its first collapse and starts a cycle of linear growth with time followed by sudden and periodic collapses. Unlike the initial growth, the secondary growths closely follow Eq. (6), i.e., no bubble burst at the top of the foam. As mentioned by Hartland and Barber (1974), below a certain height (i.e., 200 mm) the foam appeared to be stable and the collapse stopped when this height is reached and the foam starts growing again. It is believed that the 200 mm layer of stable foam acts as a cushion for the upper part and absorbs the agitation at the foam/liquid interface created by the rising bubbles. As a consequence to this "cushion", the upper part of the foam can grow without being affected by the agitation at the liquid/foam interface. The foam grows like in a transient of type 1 and follows Eq. (6). When the first bubble bursts, it makes the unstable part of the foam collapse in a chain reaction down to 200 mm. The fact that at each growth the foam reaches a higher and higher thickness was attributed to the washing of dust and impurities on the tube walls that previously prevented the foam from growing (Hartland & Barber, 1974).

5. Conclusions

This paper presents a simple, experimentally validated approach to analyze the transient formation of a foam layer produced by injecting gas bubbles into a foaming solution. Three different regimes in the transient growth of the foam have been identified as a function of the superficial gas velocity: (i) at low superficial gas velocities, the foam thickness increases linearly with time and quickly reaches a steady state, (ii) at intermediate superficial gas velocities, the foam thickness exhibits large oscillations with time and never reaches a steady state, and (iii) at large superficial gas velocity, the foam thickness initially increases linearly and then suddenly collapses into a steady-state froth. The proposed model is based on the mass conservation equation for the gas phase in the foam combined with three different models for the average porosity: (1) a constant average porosity of 0.82, (2) an exponential variation of average porosity with time, and (3) an approximate solution of the drainage equation. This model enables one to better understand the physical mechanisms that occur during the foam formation

and the effects of the superficial gas velocity on the foam dynamics. The present analysis provides the framework for more fundamental and detailed studies of the foam formation and leads to the following conclusions:

(1) For practical calculations, a linear model given by Eq. (6) with a constant average porosity equal to 0.82 can be used. The model predictions show very good agreement with experimental data for low superficial gas velocity and provide an upper limit for the foam thickness in the case of an intermediate and large superficial gas velocity.
(2) In most of the experimental data used in the present work interbubble gas diffusion can be neglected. However, we also observed that for gases with large solubility in the liquid phase, interbubble gas diffusion could play an important role and should be accounted for. Thus, further experimental and modelling work is needed to better understand the effect of interbubble gas diffusion on the transient foam thickness.When the gas solubility in the foaming solution is high, the Ostwald ripening effect becomes dominant especially when the bubble size is small and the bubbles are polydispersed. In this case, the interbubble mass transfer becomes significant, and the proposed model may not be valid.
(3) In the case of intermediate superficial gas velocity featuring large transient oscillations of the foam thickness, two different mechanisms could be suggested to explain the foam dynamics. The first bubble bursting at the top of the foam generates either (1) a high-velocity liquid jet that breaks up into a number of small drops, or (2) a pressure wave (detonation) propagating through the foam. Both mechanisms cause the bubbles sufficiently drained to burst in a chain reaction and explain qualitatively the experimental observations. However, more careful observations and measurements have to be performed in order to experimentally validate these mechanisms. The addition of salts to a surfactant solution and the Gibbs–Marangoni effect may have a profound effect on the film/interface stability, and this effect on the dynamics of the foam growth needs to be further investigated.
(4) Additional work is needed on modelling the characteristic time for drainage and the lifetime of a critically thin lamellae. The mechanical effect of the disturbances at the liquid/foam interface on the total foam thickness should also be investigated.
(5) The present work also contributes to better understanding of the decay of standing foams that was proven to be very sensitive to the bubble size distribution in the foam layer at the instant the gas supply is shut off (Monsalve & Schechter, 1984); the bubble size distribution at the beginning of the foam decay can only be determined in the limit of the dynamic foam growth, which is analyzed in this paper.

Notation

A	parameter, Eq. (26)
a_i	coefficients of the polynomial expansion of $\bar{\phi}(z,t)$ in terms of z [Eq. (8)]
B	parameter, Eq. (27)
b_i	coefficients of the polynomial expansion of $\bar{\phi}$ in terms of t [Eq. (33)]
c_v	dimensionless parameter, Eq. (3)
g	specific gravity
H_∞	steady-state thickness
$H(t)$	transient foam thickness
j	superficial gas velocity
j_m	superficial gas velocity for onset of foaming
m	mass
q_{PB}	mass flow rate through the Plateau border
r	local bubble radius in the foam
r_0	average bubble radius in the foam
R	universal gas constant $=8.314$ J/mol K
S	cross-sectional area of the container
t	time
z	downward vertical elevation (see Fig. 2)

Dimensionless numbers

Ca	Capillary number, defined in Eq. (18)
Fr	Froude number, defined in Eq. (18)
Re	Reynolds number, defined in Eq. (18)

Greek letters

α	parameter, $=\sqrt{0.644}/0.322$, Eq. (3)
ϕ	foam porosity (volumetric gas fraction)
$\bar{\phi}(t)$	average foam porosity
ϕ_1	porosity at the top of the foam
ϕ_2	porosity at the bottom of the foam
μ	dynamic viscosity
ρ	density
σ	surface tension
τ	characteristic time required to reach steady-state conditions
τ_c	lifetime of the critically thin film
τ_d	characteristic time for drainage

Subscripts

g	refers to gas
max	refers to the maximum value
min	refers to the minimum value

Acknowledgements

This work was supported by the U.S. Department of Energy/Glass Industry/Argonne National Laboratory/ University collaborative research project. The authors are

indebted to Dr. G. Narsimhan and to the glass industry representatives for helpful discussions and exchange of information. The authors would also like to acknowledge the comments of anonymous referees on the validity of the boundary condition, Eq. (11), and on the importance of various effects on the foam dynamics and stability that resulted in a significant improvement of the final manuscript.

References

Barber, A. D., & Hartland, S. (1975). The collapse of cellular foams. *Transactions of the Institution of Chemical Engineers*, *53*, 106–111.

Bhakta, A., & Ruckenstein, E. (1995). Drainage of standing foam. *Langmuir*, *11*, 1486–1492.

Bhakta, A., & Ruckenstein, E. (1997). Decay of standing foams: Drainage, coalescence and collapse. *Advances in Colloid and Interface Science*, *70*, 1–124.

Boulton-Stone, J. M., & Blake, J. R. (1993). Gas bubbles bursting at a free surface. *Journal of Fluid Mechanics*, *254*, 437–466.

Desai, D., & Kumar, R. (1982). Flow through a Plateau border of cellular foam. *Chemical Engineering Science*, *37*(9), 1361–1370.

Desai, D., & Kumar, R. (1983). Liquid holdup in semi-batch cellular foams. *Chemical Engineering Science*, *38*(9), 1525–1534.

Djabbarah, N. F., & Wasan, D. T. (1985). Foam stability: The effect of surface rheological properties on the lamella rupture. *A.I.Ch.E. Journal*, *31*(6), 1041–1043.

Fedorov, A. G., & Viskanta, R. (2000). Radiative transfer in a semitransparent glass foam blanket. *Physics and Chemistry of Glasses*, *41*(3), 127–135.

Germick, R. J., Rehill, A. S., & Narsimhan, G. (1994). Experimental investigation of static drainage of protein stabilized foams—comparison with model. *Journal of Food Engineering*, *23*, 555–578.

Hartland, S., & Barber, A. D. (1974). A model for cellular foam. *Transactions of the Institution of Chemical Engineers*, *52*, 43–52.

Hartland, S., Bourne, J. R., & Ramaswami, S. (1993). A study of disproportionation effects in semi-batch foams—II. Comparison between experiment and theory. *Chemical Engineering Science*, *48*, 1723–1733.

Hrma, P. (1990). Model for a steady state foam blanket. *Journal of Colloid and Interface Science*, *134*(1), 161–168.

Hutzler, S., Weaire, D., & Shah, S. (2000). Bubble sorting in a foam under forced drainage. *Philosophical Magazine Letters*, *80*(1), 41–48.

Jeelani, S. A. K., Ramaswami, S., & Hartland, S. (1990). Effect of binary coalescence on steady-state height of semi-batch foams. *Transactions of the Institution of Chemical Engineers*, *68*(Part A), 271–277.

Kappel, J., Conradt, R., & Scholze, H. (1987). Foaming behavior on glass melts. *Glastechnische Berichte*, *60*(6), 189–201.

Krotov, V. V. (1981). Theory of syneresis and foams and concentrated emulsions. 3. Local equation of syneresis and formulation of boundary conditions. *Colloid Journal of the USSR*, *43*, 33–39.

Laimbock, P. R. (1998). *Foaming of glass melts*. Ph.D. thesis, Technical University of Eindhoven, Eindhoven, The Netherlands.

Malysa, K. (1992). Wet foams: Formation, properties and mechanism of stability. *Advances in Colloid and Interface Science*, *40*, 37–83.

Monsalve, A., & Schechter, R. S. (1984). The stability of foams: Dependence of observation on the bubble size distribution. *Journal of Colloid and Interface Science*, *97*(2), 327–335.

Narsimhan, G. (1991). A model for unsteady state drainage of a static foam. *Journal of Food Engineering*, *14*, 139–165.

Narsimhan, G., & Ruckenstein, E. (1986a). Effect of bubble size distribution on the enrichment and collapse in foams. *Langmuir*, *2*, 494–508.

Narsimhan, G., & Ruckenstein, E. (1986b). Hydrodynamics, enrichment, and collapse in foams. *Langmuir*, *2*, 230–238.

Ozturk, B., & Fruehan, R. J. (1995). Effect of temperature on slag foaming. *Metallurgical and Materials Transactions B*, *26B*, 1086–1088.

Pattle, R. E. (1950). The control of foaming. II. The breakdown mechanisms and volume of dynamic foams. *Journal of the Society of Chemical Industry*, *69*, 368–371.

Pilon, L., Fedorov, A. G., & Viskanta, R. (2001). Steady-state foam thickness of liquid-gas foams. *Journal of Colloid and Interface Science*, *242*, 425–436.

Ramaswami, S., Hartland, S., & Bourne, J. R. (1993). A study of disproportionation effects in semi-batch foams—I. Simulation of bubble size distribution. *Chemical Engineering Science*, *48*, 1709–1721.

Ramkrishna, D. (2000). *Population balances*. San Diego, CA: Academic Press.

Tenenbaun, M., & Pollar, H. (1963). *Ordinary differential equations*. New York, NY: Harper & Row.